Effect of Si adsorption on the atomic and electronic structure of Au_n clusters ($n=1-8$) and the Au (111) surface: First-principles calculations

Chiranjib Majumder*
Chemistry Division, Bhabha Atomic Research Center, Trombay, Mumbai 400 085, India
(Received 1 February 2007; published 6 June 2007)

The interaction of silicon atoms with finite-size gold clusters and the periodic slab of the Au (111) surface have been investigated using the density-functional theory formalism. The projector augmented wave method under the spin-polarized version of the generalized gradient approximation scheme was employed to calculate the total energy. For clusters, it is found that the interaction of Si atom results in an early onset (from $n=3$ onwards) of three-dimensional structures. This is different from the behavior observed for $3d$ or $5d$ metal atoms, which retains the planar conformation of Au clusters. The reason for such shift in the structural motif is attributed to the significant contribution of the p electrons of Si, resulting in strong directional covalent bonding. Based on the energetics, the $SiAu_4$ cluster has been found to show extraordinary stability in this series. From the ground-state geometries of larger size $SiAu_n$ ($n>4$) clusters, it is realized that the coordination of Si saturates at 4 and the geometrical changes induced in the Au host are localized. For the interaction of Si atom on the Au (111) periodic slab, an hcp hollow site was found to be the most favored adsorption site. The charge distribution analysis showed finite charge transfer from Si to the Au host, resulting in a shift of the Fermi level upwards. Finally, a comparison of Si interaction between cluster and periodic slab models reveals that although there is difference in the absolute magnitude of interaction energy and the geometrical parameters, in both systems, the inherent bonding is found to be covalent in nature.

DOI: 10.1103/PhysRevB.75.235409 PACS number(s): 73.22.−f, 36.40.Cg, 36.40.Ei, 36.40.Qv

INTRODUCTION

During the past few years, gold clusters have attracted the attention of a wide range of researchers. Apart from the fundamental understanding of the finite-size effect, the interest on gold clusters is primarily based on its various applications such as molecular electronic devices, catalyst, biological diagnoistics, etc.[1–18] Based on theoretical investigations, Häkkinen *et al.*[10] have predicted that Au_N^- clusters favor planar configurations for considerably larger size, which is strikingly different than what has been observed for most of the metal clusters. These predictions were further verified by Furche *et al.*[19] and Häkkinen *et al.*[20] from a combined experimental and theoretical study, which, for the first time, provided evidence that a structural transition of Au_n^- clusters from two dimensional to three dimensional occurs at 12 atoms. Recent theoretical study by Fernández *et al.*[21] predicted unusual planar structures of Au_n clusters up to $n=11$. The planarity of gold clusters is attributed to the strong relativistic effects, which enhance the *s-d* hybridization by shrinking the size of the $6s$ orbital. The photofragmentation studies carried out for Au_n clusters showed enhanced stability for specific-size clusters, which follows the electron shell-model approach or in other words, indicates the delocalization of valence electrons in these clusters.[22]

Doped clusters are important as they can be tuned for the tailored physicochemical properties. Recently, a considerable amount of experimental and theoretical work has been carried out on Au clusters doped with an impurity atom.[23–40] Most of these studies have focused on the interaction of transition-metal atom as an impurity atom. The evidence of enhanced stability for specific cluster sizes has been explained based on the shell-model approach assuming the delocalization of valence electrons. It is found that the electrons are itinerant and they follow the 18-electrons rule even in the presence of a transition-metal atom. In this series, Au_5X^+ ($X=Cr,Mn,Fe,Co,Zn$) clusters showed some extra stability, which was explained based on the structural planarity and six delocalized electrons being a magic number for two-dimensional systems.[29,30] Further, the unusual high stability of Au_5Zn^+ cluster was attributed to the sigma aromaticity, which results due to the strong magnetic shielding inside and above the structure.[31] It may be noted that in all these studies, the ground-state geometry of the Au clusters remained planar even after doping it with an impurity atom.

The versatility in the chemical nature of Au has been verified by its complex formation with a variety of elements. The unusual interaction of inert gas atom with Au was addressed by Pyykko *et al.*[41] In a recent microwave spectroscopy study, the [KrAuF] species is observed and the Kr-Au bond has been identified as weakly covalent using the MP2 level of calculation.[42] In another interesting study, halogenlike behavior of Au atoms was observed in MAu_4 cluster where $M=Ti$, Hf, Zr, Th, and U. In these clusters, Au carries a formal charge of −1 and acts as a ligand to the metallic center.[32] The hydrogenlike behavior of Au atoms is reported by Boggavarapu *et al.*[43] The analogy between the SiH_4 and $SiAu_4$ was verified using the photoelectron spectroscopy and theoretical studies.

Although a large number of experimental and theoretical studies reported the electronic and geometric structures of transition-metal atom doped gold clusters, only a few have focused on the interaction of non transition elements, in particular, how they can influence the ground-state properties of gold clusters. Apart from the chemistry between silicon and gold, silicon being an important element in the field of nanoelectronics, it is of our interest to study the interaction of Si atoms on the Au surface. For this purpose, we have mod-

eled the Au surface by a finite-size cluster and an infinite slab. The primary objective of this study is to understand the silicon atom interaction on the geometrical and electronic structures of free gold clusters and an infinite slab. Therefore, this study will reveal two important aspects: (i) the fundamental aspect of the structure and bonding of Au_nSi clusters and (ii) how the adsorption of Si atoms changes from finite-size clusters to the infinite-size slab of the Au (111) surface.

COMPUTATIONAL DETAILS

The geometry optimization of several isomeric structures was performed using the density-functional theory formalism as implemented in VASP.[44] The total-energy calculation was carried out based on plane-wave expansion method employing scalar relativistic ultrasoft pseudopotentials and the spin-polarized version of the generalized gradient approximation (GGA) for exchange and correlation.[45] A simple cubic cell of 15 Å dimension with the Γ point for the Brillouin-zone integration was considered for these calculations. The geometries are considered to be converged when the force on each ion becomes 0.01 eV/Å or less. The cutoff energy for the plane-wave basis set was 300 eV. The total-energy convergence was tested with respect to the plane-wave basis set size and simulation cell size, and the total energy was found to be accurate to within 1 meV.

RESULTS AND DISCUSSION

In order to test the performance of the computational method employed in the present investigation, it is important to compare the results with previously published studies. For this purpose, we have used Au_2 and AuSi dimers as reference systems to check the reliability of the computational strategy and the atomic pseudopotentials used in this work. A comparison between the calculated and experimental values of the binding energy and bond lengths of these dimers is listed in Table I. The optimized bond length of Au_2, Au-Si, and Si_2 is found to be 2.53, 2.25, and 2.28 Å, respectively, and the binding energy follows the trend as $Si_2 > Au\text{-}Si > Au_2$. Excellent agreement between the measured and calculated values suggests the reliability of the theoretical method employed in this work. Moreover, the higher binding energy of Au-Si in comparison to that of Au_2 indicates the presence of strong covalent bonding between Au and Si atoms.

TABLE I. Theoretical and experimental (Ref. 46) binding energies and bond lengths of the dimers used in this work.

	B.L. (Å)		BE/atom (eV)	
System	Calc.	Expt.	Calc.	Expt.
Au_2	2.52	2.47	1.155	1.16
Au–Si	2.25		1.71	1.58
Si_2	2.28	2.24	1.77	1.66

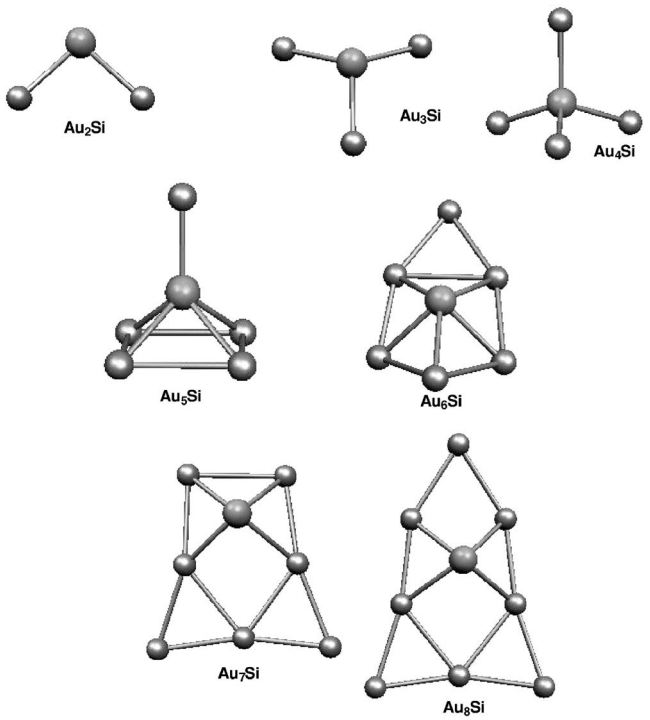

FIG. 1. Lowest-energy isomers of Au_nSi ($n=2-8$) clusters.

Geometries of Au_nSi ($n=2-5$)

The lowest-energy configuration of Au_2Si cluster forms an isosceles triangle with Au-Au and Au-Si distances of 3.31 and 2.27 Å, respectively (Fig. 1). We note that the Au-Au distance in Au_2Si has increased significantly compared to that in Au_2 dimer. The angle between Au-Si-Au is found to be 93°. The binding energy calculated for the isosceles Au_2Si triangle is found to be 2.03 eV/atom. This is significantly larger than the binding energy of Au_3 cluster. The additional energy is due to the stronger interaction between Au and Si atoms. The Au_3Si cluster consisting of four atoms is interesting as this is the smallest cluster to show its preference of choice towards two-dimensional (2D) or three-dimensional (3D) structural isomers. Previous studies on pure[19–22] and transition-metal impurity doped gold clusters suggested that, at least up to hexamer ($n=6$), they favor planar configurations. Most remarkably, we find a three-dimensional capped triangle with C_{3v} point symmetry as the lowest-energy isomer for Au_3Si cluster. The Au-Si bond lengths are found to be 2.27 Å and the angle between Au-Si-Au is found to be 112°. The reason for such early 3D structural motif in Au_nSi cluster is attributed to the directional covalent bonding of the Au-Si bonds. In fact, the geometrical features of the Au_3Si cluster resemble well that of NH_3 molecule, where the sp^3 hybridization is responsible for the nonplanarity. The next higher-energy isomer shows a bent rhombus structure, which is 0.186 eV higher in energy. The planar isomers of the Au_3Si cluster are found to be significantly higher in energy. For Au_4Si cluster, the lowest-energy isomer shows tetrahedral configuration which is very similar to that of CH_4 methane molecule. The binding energy of the Au_4Si is found to be 2.38 eV/atom and the energy gap between the highest occu-

pied molecular-orbital and lowest unoccupied molecular-orbital energy levels is estimated to be 2.1 eV. This is in good agreement with the experimental gap of 2.36 eV,[27] considering the fact that usually, GGA underestimates the gap. The Si-Au bond length is found to be 2.27 Å and the angle between Au-Si-Au is 109°. Another isomer, with square prism structure (C_{4v}), is 0.227 eV higher is energy. The W shaped planar isomer is found be 0.30 eV higher in energy. It should be mentioned that the pure Au_5 cluster shows the planar W shaped configuration as the lowest-energy isomer. The preference of 3D structural growth reflects the covalent bonding due to the sp^3 hybridization. Recently, a large number of experimental and theoretical studies have been carried out on Au_5X clusters,[31–36] where X represents an impurity atom. The ground-state geometry of all these Au_5X clusters showed that it favors the planar structure like Au_6 cluster, where the valence electrons of the Au and X atoms are delocalized. However, it is to be noted that in these studies, the X atoms were chosen to be a transitional-metal atom and the interaction between d electrons and Au clusters was investigated. In a very recent study, we have shown that when Au clusters interact with impurity elements through p electrons, a significant structural transition to the three-dimensional geometry occurs.[33] It is found that the lowest-energy isomer of the Au_5Si favors a top capped square prism structure with C_{4v} symmetry. A capped tetrahedron where the additional Au atom caps the threefold coordination site of the Au_4Si from the outside is just 0.018 eV higher in energy. The small energy difference between these two isomers suggests that a switchover between these two isomers is possible at higher temperature or by using a different theoretical method.

Geometries of Au_nSi ($n=6-8$)

The heptamer clusters of coinage group elements are important as significant structural and bonding differences are reported between copper, silver, and gold clusters. Previous calculations show that while Au clusters remain planar up to $n=11$,[21] both copper[47–50] and silver[51] clusters show 2D to 3D structural transition from the heptamer onward. So far, a large number of experimental and theoretical studies have been carried out to investigate the structure and bonding of transition-metal atom doped Au_6 clusters. The results showed that the ground-state structure Au_6X (X=transition-metal atom) remains planar even after doping with transition-metal elements.[38] Few studies are available on the interaction of Si atom with small Au clusters, and so far, they are limited up to $n=5$. The Si atom interaction with Au_6 cluster or larger is important for two reasons. The first one is to understand the effect of the localized covalent bonding on the second neighboring Au atoms. Secondly, the Au_6 forms a very stable planar structure with triangular atomic arrangement similar to that of Au (111) surface and therefore, it can be used as a two-dimensional model of the infinite surface in a finite-size limit. Here, a large number of two- and three-dimensional geometries were optimized to obtain the lowest-energy isomer of the Au_6Si cluster. It is found that there are a large number of local minima existing in the potential-energy surface of the Au_6Si cluster, and more importantly, all of them favors nonplanar structures. For larger clusters, the structural trend of Au_7Si and Au_8Si clusters follows the Au_6Si growth motif. In particular, it is found that Si atoms bind at the four coordination site on Au clusters and all Au atoms of the host cluster are inclined to remain in the planar configurations. A few low-lying isomers of Au_6Si, Au_7Si, and Au_8Si clusters along with the energy differences with respect to the lowest-energy isomer are listed in Ref. 52

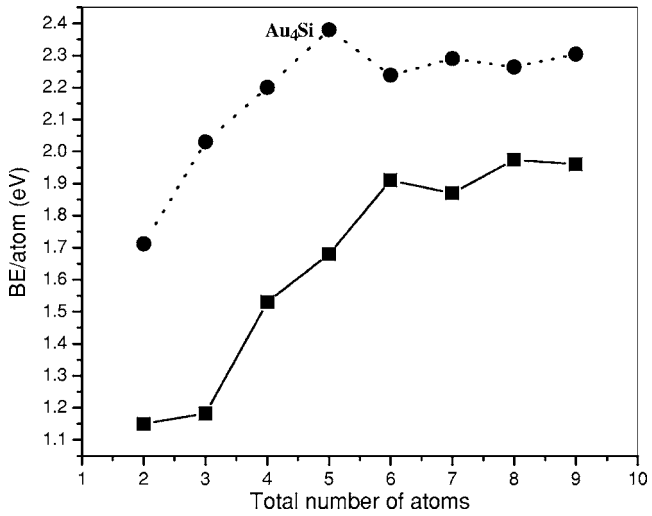

FIG. 2. The average binding energy of Au_n (square) and Au_nSi (circle) clusters ($n=1-8$).

Energetics

The stability of Au_n and Au_nSi clusters is compared based on their average binding energy, calculated as

$$\mathrm{BE}(\mathrm{Au}_n) = 1/n[E(\mathrm{Au}_n) - nE(\mathrm{Au})],$$

$$\mathrm{BE}(\mathrm{Au}_n\mathrm{Si}) = 1/(n+1)[E(\mathrm{Au}_n\mathrm{Si}) - nE(\mathrm{Au}) - E(\mathrm{Si})].$$

The binding energy of Au_n and Au_nSi clusters as a function of the total number of atoms present in the cluster is plotted in Fig. 2. It is clear that the substitution of Au by Si leads to improvement of the overall binding. This is due to the higher bond strength of the Au-Si than that of Au-Au, 1.71 and 1.15 eV, respectively. For Au_n clusters, up to $n=6$, the binding energy is found to increase as a function of cluster size with small oscillations for odd and even numbers of valence electrons present in the cluster. Unlike this, the binding energy of Au_nSi clusters shows a sharp increase up to $n=4$, followed by a dip at $n=5$. These features clearly indicate the higher stabilities of Au_6 and Au_4Si clusters in the series of Au_n and Au_nSi clusters, respectively.

The relative stability order in a series of clusters can be illustrated more emphatically through the second-order energy difference as a function of cluster size, as shown in Fig. 3. It is found that the stability pattern of Au_n and Au_nSi clusters follows the same trend and the details of the relative stability depending on the number of Au atoms present in the cluster. For example, $n=2$, 4, and 6 show higher stability

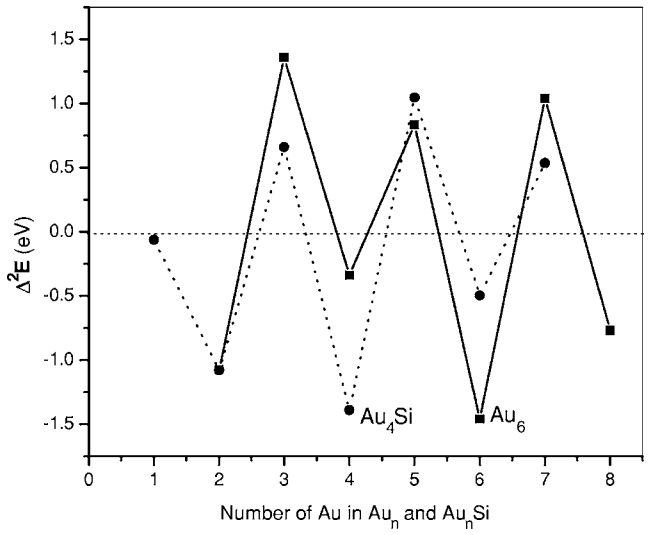

FIG. 3. Second-order difference in total energy ($\Delta^2 E$) of Au_n (square) and Au_nSi (circle) ($n=2-8$) clusters as a function of size.

over others for both Au_n and Au_nSi clusters. The large negative values of the $\Delta^2 E$ for Au_6 and Au_4Si further establish their magical stability in these series of clusters.

Incremental atom attachment energy is another important parameter to describe the stability or, in turn, the bond strength of the last atom with that of the host clusters. The attachment energy of Au with Au_{n-1} and $Au_{n-1}Si$ is estimated by using the following equations:

$$\Delta E(\text{Au on Au}_{n-1}) = E(\text{Au}_n) - E(\text{Au}_{n-1}),$$

$$\Delta E(\text{Au on Au}_{n-1}\text{Si}) = E(\text{Au}_n\text{Si}) - E(\text{Au}_{n-1}\text{Si}).$$

Figure 4 shows the attachment energy of Au on the Au_n and Au_nSi clusters as a function of cluster size. In general, both

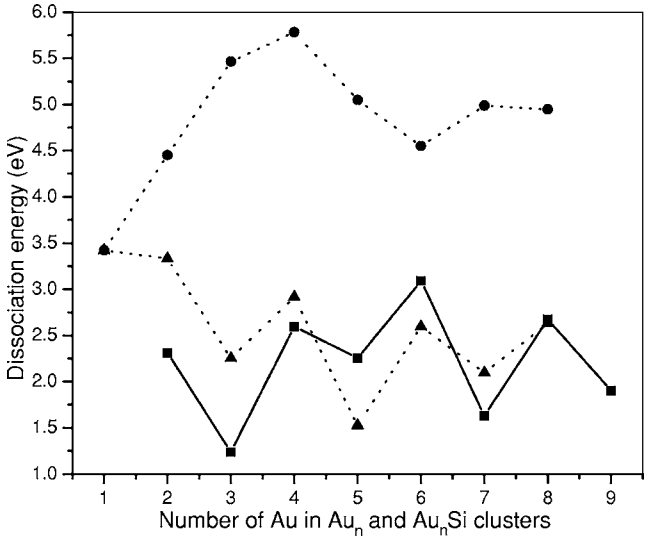

FIG. 4. The attachment energy of Au and Si atoms with Au_n clusters. While squares and triangles represent the Au attachment energy with $Au_{(n-1)}$ and $Au_{(n-1)}Si$ clusters, circles represent the Si atom attachment energy with Au_n clusters.

curves show similar trend in the stability pattern, i.e., odd-even alternation of Au attachment energy is observed for both Au_n and Au_nSi series of clusters. However, an interesting difference has been noticed in the details of the Au attachment energy between Au_n and Au_nSi clusters. For $n<5$, it is found that the dissociation of Au from Au_nSi requires more energy than that from Au_n clusters. The trend reversed for $n=5$ and 6. The reason for such trend can be attributed to the strong covalent bonding of Si with Au atoms, which saturates at $n=4$ coordination. For Au_5Si and Au_6Si clusters, Si binds with five Au atoms and thereby reduces the bond strength of each Au-Si bond which is responsible for the lower dissociation energy of Au from these clusters. For Au_7Si and Au_8Si clusters, Si binds with four Au atoms and the additional Au atoms are connected through already bonded Au atom with Si, and therefore, the dissociation energy of the Au-Au bond is similar that of Au_n clusters.

Further, we have calculated the Si atom attachment energy $[\Delta E(\text{Si on Au}_n) = E(\text{Au}_n\text{Si}) - E(\text{Au}_n) - E(\text{Si})]$ with Au_n clusters. In contrast to the oscillatory behavior observed for Au, the attachment energy of the Si atom show continuous increase up to $n=4$ and then follows a decreasing trend. This stability pattern clearly indicates the difference in binding of Si in comparison to that of Au atom. The large attachment energy of Si atom is due to the higher binding strength of Si with Au clusters which ranges from 3.42 to 5.70 eV. The magic behavior of Au_4Si cluster can be explained due to the covalent nature of bonding through sp^3 hybridization. Consequently, the energy ordering of Au clusters is expected to be changed by the influence of Si atom.

In order to understand the chemical bonding in these clusters, we have analyzed the electron-density distribution and reordering of the electronic energy levels. The density of states (DOS) provides a convenient overall view of the cluster electronic structure. Figure 5 shows a representative DOS spectrum for Au_n and Au_nSi ($n=2$, 4, 6, and 8) clusters. The DOS is obtained by broadening the one-electron Kohn-Sham electronic energies of the lowest-energy isomers with the 0.1 Gaussian. The comparison of the DOS between Au_n and Au_nSi clusters suggests that, in general, the energy levels of the Au_nSi clusters are shifted upwards (less $-ve$) with respect to that of pure Au_n spectrum. The reason for such shift can be attributed to the electronic charge injection from the Si levels to the Au clusters. To verify this fact, we have further analyzed the electronic charge distribution of Au_nSi clusters. This has been obtained by expanding the wave function into angular momentum components within spheres of radius of 1.6 and 1.4 for Au and Si atoms, respectively. As significant charge lies outside the spheres, this decomposition is only representative and is expected to give a qualitative picture of the charge distribution. Based on this calculation, it has been found that the Si atom transfers finite electronic charge to the Au_n host. Now, to underline the charge transfer in a more specific way, we have analyzed the difference of orbital-decomposed charges before and after interaction of Au_n clusters with Si atom. The results reveal that (shown in Table II) while there is an increase in the electronic charge in the s and p orbitals, the density of the d-orbital electrons remain unaltered. Thus, it may be inferred that the chemical bonding of these clusters are primarily governed through s and p-orbital

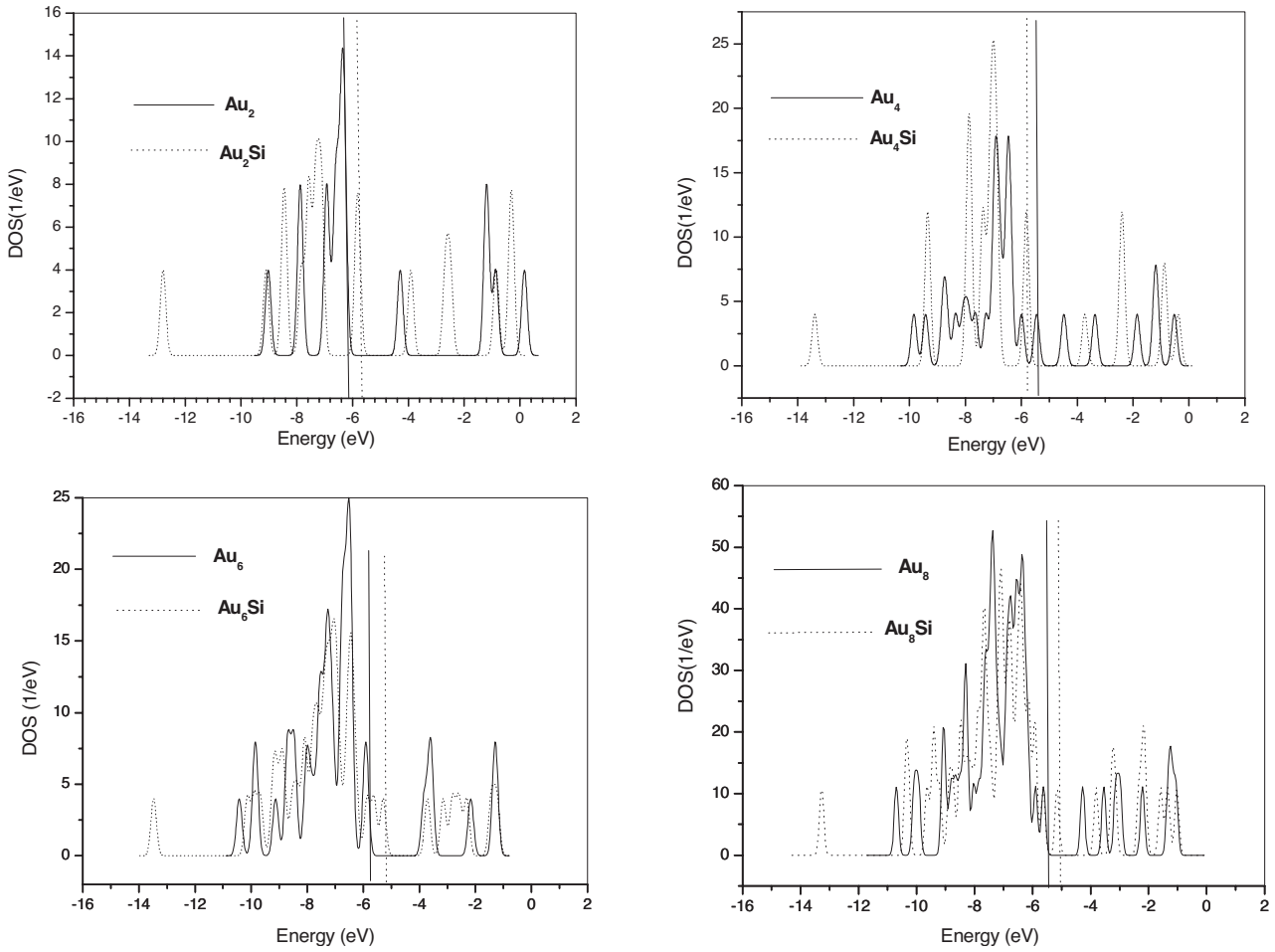

FIG. 5. Electronic density of states of (a) Au_n and (b) Au_nSi ($n=2$, 4, 6, and 8) clusters. The one-electron Kohn-Sham energies have been broadened with a 0.01 eV Gaussian.

interactions which are also responsible for an early onset of nonplanar geometries.

The adsorption of Si atom on the Au (111) surface

A cluster of metal atoms, representing an extended substrate, has been used to model the metal-molecule interactions relevant for catalysis.[53] However, cluster models are limited due to the finite-size effects, and therefore, the results may differ considerably from a realistic point of view. In this work, our objective is to underscore the differences in the nature of interaction of the Si between a cluster and a slab model of the Au (111) surface. In previous sections, we have discussed the geometries and energetics of Si atom doped Au clusters. To begin with the slab model, test calculations were performed on the structural and electronic properties of the Au bulk. The lattice constant of the fcc solid was found to be 4.12 Å, which is in good agreement with the experimental value of 4.08 Å.[54] The Au (111) surface has been modeled by truncating the infinite bulk surface in the X-Y direction with four layers in the Z direction. For the optimization of this slab, while the atomic positions of the top three layers were optimized, the atoms at the bottom layer were kept fixed at the bulk values. In particular, we have used two different slab

TABLE II. A comparison of the orbital-decomposed electronic charge distribution between Au_n and Au_nSi clusters. While columns 2–4 represent the total charges in the s, p, and d orbitals of Au_n clusters, columns 6–8 represent the orbital charges on the Au atoms in Au_nSi clusters.

System	s	p	d	System	s	p	d
Au_2	1.57	0.20	18.72	Au_2 in Au_2Si	2.22	0.312	18.44
Au_4	3.23	0.92	37.30	Au_4 in Au_4Si	3.63	1.147	37.23
Au_6	5.09	1.63	55.89	Au_6 in Au_6Si	5.43	1.86	55.70
Au_8	5.93	1.73	73.90	Au_8 in Au_8Si	7.316	2.68	74.217

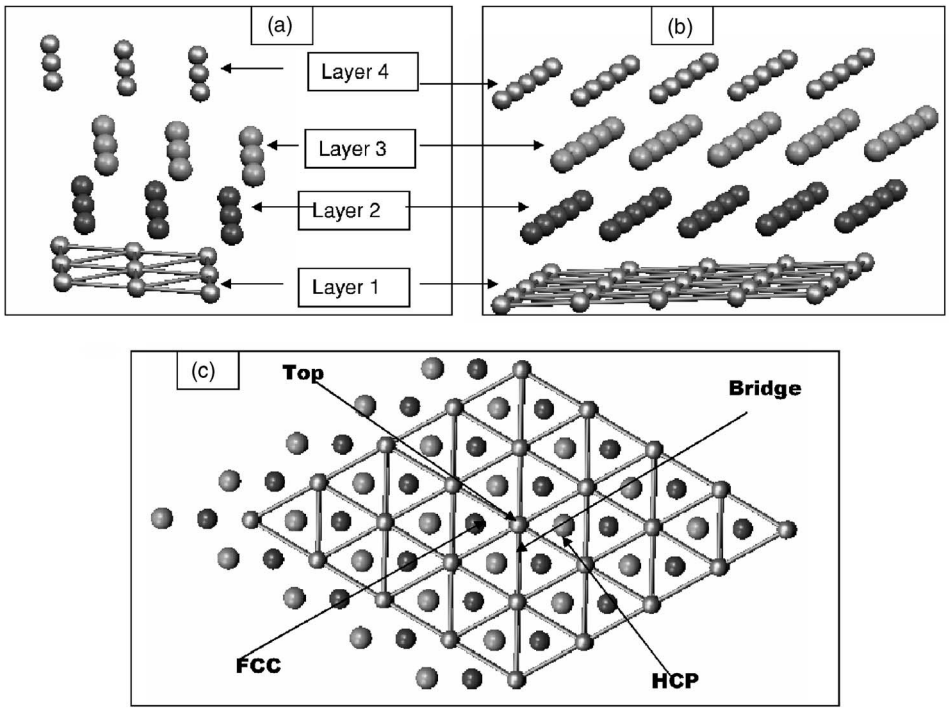

FIG. 6. (a) and (b) show the side view of the $3\times3\times4$ and $5\times5\times4$ slab models, respectively. (c) shows the top view of the $5\times5\times4$ slab model. The four well-defined adsorption sites of the surface are depicted by the arrow marks.

models, the first one with 3×3 and the second one with 5×5 atoms in the plane. Four vertical layers have been used in both cases. Two neighboring slabs were separated by 12 Å in the Z direction. The initial structures of the $3\times3\times4$ and $5\times5\times4$ slabs are shown in Fig. 6. A Monkhorst-Pack K point mesh of size of $5\times5\times1$ was used for all geometry optimization.

In order to obtain the most preferred Si adsorption site on the Au (111) surface, the geometry optimization was carried out at two different levels. In the first level, the Si atom was placed at four well defined sites of the Au (111) surface (top, bridge, hcp, and fcc), as shown in Fig. 6. In the second level, the Si atom was placed randomly at a height of 3.0 Å from the topmost layer of the Au (111) surface and allowed to relax. It may be noted that while the first four relaxations are biased, the last one is unbiased to any specific site. After relaxation of all possible geometries, a good agreement between the lowest-energy structures from levels I and II was obtained, which suggests that Si atom favors to occupy the threefold hcp site on the Au (111) surface. The energetics of the Si atom adsorption on the Au (111) surface is summarized in Table III. It is clear from this table that the Si atom adsorption energy does not change by increasing the supercell length. However, it should be mentioned that the adsorption energy of the Si atom on the slab model is smaller than that in the case of the cluster model. The reason for such difference could be due to the restraint imposed on the relaxation of the slab in comparison to that of a cluster.

TABLE III. The adsorption energy $[E_{ad}=E_{(slab+Si)}-E_{slab}—E_{Si}]$ of the Si atom at different adsorption sites on the Au (111) surface.

Model	Top (eV)	Bridge (eV)	hcp (eV)	fcc (eV)	Free fall (eV)
$3\times3\times4$	2.35	3.01	4.24	4.15	4.24
$5\times5\times4$					4.22

The lowest-energy structure shows that Si atom is at a height of 1.77 Å from the top layer of the $3\times3\times4$ slab model. The smallest interatomic distance between the Au and Si is found to be 2.43 Å. Similar geometrical arrangements were found when the Si atom was relaxed on the $5\times5\times4$ slab model. At this point it, may be interesting to compare the interfacial geometries of the Si atom interaction between cluster and surface models. For this purpose, we have summarized (Table IV) the geometrical parameters of the Au_3Si clusters and the local geometry at the site of Si atom adsorption on the Au (111) surface. From Table IV, it is found that for Au_3Si cluster, while the interatomic separations between the Au atoms are much longer, the Au-Si distance is shorter than in the slab model, which, in turn, suggests improved interaction energy for the cluster model. Moreover, for the Au_3Si cluster, the angle between the Au-Si-Au atoms is found to be close to 109°, which further suggests strong sp^3 hybridization between Au and Si atoms in the case of the cluster model. These two reasons may be attributed to the larger adsorption energy found in the case of the cluster model over the slab model.

CONCLUSION

In this work, we have reported the geometry and energetics of the finite-size Au_nSi clusters and Si atom adsorption on

TABLE IV. Comparison of the geometrical parameters and adsorption energies (E_{ad}) of the Si atom adsorption between the cluster (Au_3Si) and slab models.

	Au-Si (Å)	Au-Au (Å)	<Au-Si-Au (deg)	E_{ad} (eV)
Au_3Si	2.27	3.76	111	5.46
Si-Au (111)	2.43	3.06	78	4.24

the extended substrate of the Au (111) surface. The density-functional theory formalism under the generalized gradient approximation scheme was used to calculate the total energy of the system. The results show an early onset of nonplanar geometries of the Au_nSi clusters which is strikingly different than what is observed for transition-metal atom interactions. Whereas for transition-metal atom doping, gold cluster retains its two-dimensional geometrical shape up to $n=6$, for Si atom, interactions result in the onset of 3D structures from $n=3$ onward. The reason for the preference of nonplanar geometry of Au_nSi clusters is attributed to the involvement of *p*-orbital electrons into the bonding, which results in a strong directional covalent bond. The geometrical features of the Au_nSi clusters suggest that the effect of Si atom interaction with Au clusters is localized and the coordination number saturates at 4. This fact is further corroborated from the thermodynamic stability of these clusters, which revealed an extraordinary stability of $SiAu_4$ cluster over others in this series. The bonding analysis was carried out using the charge distribution analysis and the density of states spectrum. It has been found that a finite charge transfer occurs from Si to the *s* and *p* orbitals of Au atoms, which is responsible for the upward shift in the eigenvalue spectrum of the Au_nSi clusters in comparison to that of pure Au_n clusters.

To understand the Si atom interaction on an extended substrate, Au (111) surface has been modeled by a periodic four layer slab and the geometries were optimized by placing the Si atoms at different adsorption sites. It is found that Si atom prefers to adsorb on the hcp site over other well defined sites. The comparison of adsorption energy between the cluster and slab models indicates higher interaction energy on the bare cluster. The reason for such difference is the restraint imposed on the relaxation of the slab in comparison to that of a cluster. Although there is significant difference in the absolute magnitude in the interaction energy and the geometrical parameters, the chemical bonding between Si and Au atoms as found to govern through covalent interactions for both cluster and slab models.

ACKNOWLEDGMENT

The author is thankful to the members of the Computer Division, BARC, for their continuous support and the use of the ANUPAM supercomputing facility.

*chimaju@barc.gov.in

[1] R. L. Whetten, J. T. Khoury, M. M. Alvarez, S. Murthy, I. Vezmar, Z. L. Wang, P. W. Stephens, C. L. Cleveland, W. D. Luedtke, and U. Landman, Adv. Mater. (Weinheim, Ger.) **5**, 8 (1996).

[2] R. P. Andres, T. Bein, M. Dorogi, S. Feng, J. I. Henderson, C. P. Kubiak, W. Mahoney, R. G. Osifchin, and R. Reifenberger, Science **272**, 1323 (1996).

[3] C. A. Mirkin, R. L. Letsinger, R. C. Mucic, and J. J. Storhoff, Nature (London) **382**, 607 (1996).

[4] A. P. Alivisatos, K. P. Johnsson, X. G. Peng, T. E. Wilson, C. J. Loweth, M. P. Bruchez, and P. G. Schultz, Nature (London) **382**, 609 (1996).

[5] R. P. Andres, J. D. Bielefeld, J. I. Henderson, D. B. Janes, V. R. Kolagunta, C. P. Kubiak, W. J. Mahoney, and R. G. Osifchin, Science **273**, 1690 (1996).

[6] I. L. Garzón, K. Michaelian, M. R. Beltrán, A. Posada-Amarillas, P. Ordejón, E. Artacho, D. Sánchez-Portal, and J. M. Soler, Phys. Rev. Lett. **81**, 1600 (1998).

[7] I. L. Garzón, C. Rovira, K. Michaelian, M. R. Beltrán, P. Ordejón, J. Junquera, D. Sánchez-Portal, E. Artacho, and J. M. Soler, Phys. Rev. Lett. **85**, 5250 (2000).

[8] K. Michaelian, N. Rendón, and I. L. Garzón, Phys. Rev. B **60**, 2000 (1999).

[9] T. G. Schaaff and R. L. Whetten, J. Phys. Chem. B **104**, 2630 (2000).

[10] H. Häkkinen, M. Moseler, and U. Landman, Phys. Rev. Lett. **89**, 033401 (2002).

[11] J. Wang, G. Wang, and J. Zhao, Phys. Rev. B **66**, 035418 (2002).

[12] O. D. Häberien, S. C. Chung, M. Stener, and N. Rösch, J. Phys. Chem. **106**, 5189 (1997).

[13] C. L. Cleveland, Uzi Landman, Thomas G. Schaaff, Marat N. Shafigullin, Peter W. Stephens, and R. L. Whetten, Phys. Rev. Lett. **79**, 1873 (1997).

[14] C. L. Cleveland, U. Landman, M. N. Shafigullin, P. W. Stephens, and R. L. Whetten, Z. Phys. D: At., Mol. Clusters **40**, 503 (1997).

[15] H. Häkkinen and U. Landman, Phys. Rev. B **62**, R2287 (2000).

[16] C. J. Kiely, J. Fink, M. Brust, D. Bethell, and D. J. Schiffrin, Nature (London) **396**, 444 (1998).

[17] J. G. Hou, B. Wang, J. Yang, X. R. Wang, H. Q. Wang, Q. Zhu, and X. Xiao, Phys. Rev. Lett. **86**, 5321 (2001).

[18] B. Wang, X. Xiao, X. Huang, P. Sheng, and J. G. Hou, Appl. Phys. Lett. **77**, 1179 (2000).

[19] F. Furche, R. Ahlrichs, P. Weis, C. Jacob, S. Gilb, T. Bierweiler, and M. M. Kappes, J. Chem. Phys. **117**, 6982 (2002).

[20] H. Häkkinen, B. Yoon, U. Landman, X. Li, H.-J. Zhai, and L.-S. Wang, J. Phys. Chem. A **107**, 6168 (2003).

[21] E. M. Fernández, J. M. Soler, I. L. Garzón, and L. C. Balbás, Phys. Rev. B **70**, 165403 (2004).

[22] S. Neukermans, E. Janssens, H. Tanaka, R. E. Silverans, and P. Lievens, Phys. Rev. Lett. **90**, 033401 (2003).

[23] H. Myoung, M. Ge, B. R. Sahu, P. Tarakeswar, and K. S. Kim, J. Phys. Chem. B **107**, 9994 (2003).

[24] K. Koszinowski, D. Schröder, and H. Schwartz, ChemPhysChem **4**, 1233 (2003).

[25] H. Häkkinen, S. Abbet, A. Sanchez, U. Heiz, and U. Landman, Angew. Chem., Int. Ed. **42**, 1297 (2003).

[26] P. Pyykkö and N. Runeberg, Angew. Chem., Int. Ed. **41**, 2174 (2002).

[27] X. Li, B. Kiran, J. Li, H. J. Zhai, and L. S. Wang, Angew. Chem., Int. Ed. **41**, 4786 (2002).

[28] W. Bouwen, F. Vanhoutte, F. Despa, S. Bouckaert, S. Neukermans, L. T. Kuhn, H. Weidele, P. Lievens, and R. E. Silverans, Chem. Phys. Lett. **314**, 227 (1999).

[29] E. Janssens, H. Tanaka, S. Neukermans, R. E. Silverans, and P.

Lievens, Phys. Rev. B **69**, 085402 (2004).
[30] E. Janssens, H. Tanaka, S. Neukermans, R. E. Silverans, and P. Lievens, New J. Phys. **5**, 46 (2003).
[31] H. Tanaka, S. Neukermans, E. Janssens, R. E. Silverans, and P. Lievens, J. Am. Chem. Soc. **125**, 2862 (2003).
[32] L. Gagliardi, J. Am. Chem. Soc. **125**, 7504 (2003).
[33] C. Majumder, A. K. Kandalam, and P. Jena, Phys. Rev. B **74**, 205437 (2006).
[34] M. Heinebrodt, N. Malinowski, F. Tast, W. Branz, I. M. L. Billas, and T. P. Martin, J. Chem. Phys. **110**, 9915 (1999).
[35] D. W. Yuan, Yang Wang, and Zhi Zeng, J. Chem. Phys. **122**, 114310 (2005).
[36] B. R. Sahu, G. Maofa, and L. Kleinman, Phys. Rev. B **67**, 115420 (2003).
[37] C. Majumder and S. K. Kulshreshtha, Phys. Rev. B **73**, 155427 (2006).
[38] H. Tanaka, S. Neukermans, E. Janssens, R. E. Silverans, and P. Lievensa, J. Chem. Phys. **119**, 7115 (2003).
[39] K. Koyasu, M. Mitsui, A. Nakajima, and K. Kaya, Chem. Phys. Lett. **358**, 224 (2002).
[40] M. B. Torres, E. M. Fernández, and L. C. Balbás, Phys. Rev. B **71**, 155412 (2005).
[41] P. Pyykko, J. Am. Chem. Soc. **117**, 2067 (1995).
[42] J. M. Thomas, N. R. Walker, S. A. Cooke, and M. C. L. Gerry, J. Am. Chem. Soc. **126**, 1235 (2004).
[43] Kiran Boggavarapu, Xi Li, Hua-Jin Zhai, Li-Feng Cui, and Lai-Sheng Wang, Angew. Chem., Int. Ed. **43**, 2125 (2004).
[44] G. Kresse and J. Hafner, Phys. Rev. B **47**, 558 (1993); G. Kresse and J. Furthmüller, *ibid.* **54**, 11169 (1996); G. Kresse and J. Furthmüller, Comput. Mater. Sci. **6**, 15 (1996); G. Kresse and J. Hafner, Inst. Chem. Eng. Symp. Ser. **6**, 8245 (1994); G. Kresse and J. Hafner, Phys. Rev. B **49**, 14251 (1994).
[45] P. Perdew, in *Electronic Structure of Solids '91*, edited by P. Ziesche and H. Eschrig (Akademie, Berlin, 1991).
[46] *CRC Handbook of Chemistry and Physics*, 49th ed. edited by R. C. Weast (CRC, Cleveland, OH, 1969).
[47] K. A. Jackson, Phys. Rev. B **47**, 9715 (1993).
[48] C. Massobrio, A. Pasquarello, and R. Car, Chem. Phys. Lett. **238**, 215 (1995).
[49] C. Massobrio, A. Pasquarello, and R. Car, Phys. Rev. Lett. **75**, 2104 (1995).
[50] K. Jug, B. Zimmermann, P. Calaminici, and A. M. Köster, J. Chem. Phys. **117**, 4497 (2002).
[51] V. Bonacic-Koutecky, L. Cespiva, P. Fantucci, J. Pittner, and J. Koutecky, J. Chem. Phys. **100**, 490 (1994).
[52] The low-lying isomers of Au_6Si, Au_7Si, and Au_8Si clusters are shown as supporting information.
[53] J. L. Whitten and H. Yang, Surf. Sci. Rep. **218**, 55 (1996); G. Pacchioni, Heterog. Chem. Rev. **2**, 213 (1995).
[54] C. Kittel, *Introduction to Solid State Physics*, 7th ed. (Wiley, New York, 1996).